A Matrix-Isolation and Density Functional Theory Study of the Reactions of Laser-Ablated Beryllium, Magnesium, and Calcium Atoms with Methane

Tim M. Greene,*,† Dominick V. Lanzisera, Lester Andrews,* and Anthony J. Downs†

Contribution from the Department of Chemistry, University of Virginia, Charlottesville, Virginia 22901

Received February 12, 1998

Abstract: Beryllium atoms produced by laser ablation have been co-condensed with methane/argon mixtures onto a substrate at 10 K. Infrared spectroscopy has been used to identify a number of organoberyllium products, viz. CH_3BeH, CH_3BeCH_3, CH_3Be, H_2CBeH, and $HCBeH$. Assignments of the infrared absorption bands are made on the basis of ^2H and ^{13}C substitution and by comparison with frequencies supplied by DFT calculations. In the reaction of magnesium or calcium atoms with methane, the only insertion product that could be identified was the monomethyl metal hydride, CH_3MH (M = Mg or Ca).

Introduction

The first organoberyllium compound was reported in 1860 when Cahours treated the metal with ethyl iodide in a sealed tube giving a solid product later identified as EtBeI.[1] Although details of routes aimed at the preparation of organoberyllium hydrides, RBeH, have been reported more recently, only in a few cases have solvent-free compounds been isolated; they are typically subject to oligomerization and polymerization processes.[2] Thus, methylberyllium hydride appears to be formed either by the reaction of $[Me_2AlH]_n$ with an excess of $[Me_2-Be]_n$ or by the pyrolysis of $[MeBeBu^t]_n$, but is an intractable material which has been characterized only in the form of coordination complexes with donor ligands such as Et_2O or Me_3N.[2−4] The diethyl ether complex may be synthesized by the reaction of dimethylberyllium, beryllium bromide, and lithium hydride in diethyl ether; on the evidence of cryoscopic measurements, it is dimeric in benzene solution and the molecule $[MeBeH·OEt_2]_2$ is believed to contain a BeH_2Be bridging unit.[4]

To examine the monomeric species, we have employed the technique of matrix isolation to trap the product formed when a high-energy beryllium atom inserts into a C−H bond of a methane molecule. Such a stratagem has proved successful in our previous study of the species CH_3MH (M = Zn, Cd, or Hg).[5] For the more refractory atoms, laser ablation has proven extremely effective to examine the reaction between boron and methane[6] and to explore reactions of beryllium atoms with oxygen,[7] hydrogen,[8] water,[9] acetylene,[10] or HCN.[11]

We have extended these matrix-isolation experiments to detemine the response of methane to laser-ablated magnesium and calcium atoms. Methylmagnesium hydride may be prepared in tetrahydrofuran solution by mixing dimethylmagnesium and magnesium hydride but, like the beryllium diethyl ether analogue, the molecule is a dimer by virtue of possessing two bridging hydrogens.[12] The monomeric species has been prepared by photoexcitation of magnesium atoms trapped in pure methane matrices,[13] while matrix-isolation studies of a range of binary magnesium hydrides have also been reported.[14] Studies of the reaction of magnesium atoms with methane in the gas phase indicate that magnesium excited to the ^1P state reacts with methane on essentially every collision to produce MgH and CH_3.[15,16] There is no report in the literature of the synthesis of CH_3CaH, although phenylcalcium hydride has been prepared.[17] This has been achieved by co-condensing thermally evaporated metal atoms with benzene on a surface held at 77 K and then permitting the mixture to warm to room temperature.

Experimental Section

The apparatus for pulsed laser-ablation matrix-isolation spectroscopy has been described earlier.[18−20] Gas samples were prepared using

† Current address: Inorganic Chemistry Laboratory, University of Oxford, Oxford, OX1 3QR, U.K.

(1) Gilman, H.; Schulze, F. *J. Am. Chem. Soc.* **1927**, *49*, 2904−2908.

(2) (a) *Gmelin Handbook of Inorganic Chemistry, 8th ed., Organoberyllium Compounds*; Springer-Verlag: Berlin, Heidelberg, 1987; Part 1, Syst. No. 26, pp 93−104. (b) Bell, N. A. In *Comprehensive Organometallic Chemistry*; Wilkinson, G., Stone, F. G. A., Abel, E. W., Eds.; Pergamon: Oxford, 1982; Vol. 1, pp 142−144. (c) Bell, N. A. In *Comprehensive Organometallic Chemistry II*; Abel, E. W., Stone, F. G. A., Wilkinson, G., Eds.; Pergamon: Oxford, 1995; Vol. 1, pp 50−52.

(3) Bell, N. A.; Coates, G. E. *Proc. Chem. Soc.* **1964**, 59.

(4) Bell, N. A.; Coates, G. E. *J. Chem. Soc.* **1965**, 692−699. Bell, N. A.; Coates, G. E. *J. Chem. Soc. A* **1966**, 1069−1073.

(5) Greene, T. M.; Andrews, L.; Downs, A. J. *J. Am. Chem. Soc.* **1995**, *117*, 8180−8187.

(6) Hassanzadeh, P.; Hannachi, Y.; Andrews, L. *J. Am. Chem. Soc.* **1992**, *114*, 9239−9240; *J. Phys. Chem.* **1993**, *97*, 6418−6424.

(7) Thompson, C. A.; Andrews, L. *J. Am. Chem. Soc.* **1994**, *116*, 423−424.

(8) Tague, T. J., Jr.; Andrews, L. *J. Am. Chem. Soc.* **1993**, *115*, 12111−12116.

(9) Thompson, C. A.; Andrews, L. *J. Phys. Chem.* **1996**, *100*, 12214−12221.

(10) Thompson, C. A.; Andrews, L. *J. Am. Chem. Soc.* **1996**, *118*, 10242−10249.

(11) Lanzisera, D. V.; Andrews, L. *J. Am. Chem. Soc.* **1997**, *119*, 6392−6398.

(12) Ashby, E. C.; Goel, A. B. *J. Org. Chem.* **1977**, *42*, 3480−3485.

(13) McCaffrey, J. G.; Parnis, J. M.; Ozin, G. A.; Breckenridge, W. H. *J. Phys. Chem.* **1985**, *89*, 4945−4950.

(14) Tague, T. J., Jr.; Andrews, L. *J. Phys. Chem.* **1994**, *98*, 8611−8616.

(15) Breckenridge, W. H.; Umemoto, H. In *Dynamics of the Excited State*; Lawley, K. P., Ed.; Advances in Chemical Physics; Wiley: New York, 1982; Vol. 50.

(16) Breckenridge, W. H. *J. Phys. Chem.* **1996**, *100*, 14840−14855.

(17) Mochida, K.; Hiraga, Y.; Takeuchi, H.; Ogawa, H. *Organometallics* **1987**, *6*, 2293−2297.
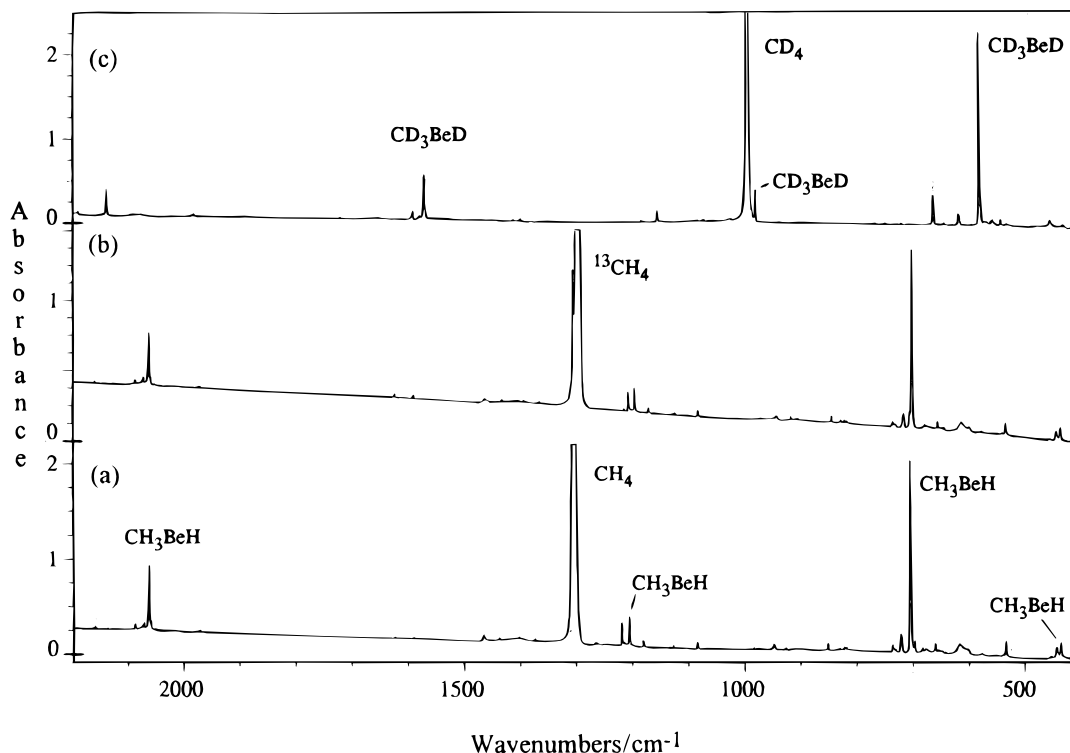
Figure 1. Infrared spectra of argon matrices following the co-deposition of laser-ablated Be atoms with 2% methane/argon mixtures at 10 K: (a) Be + CH_4, (b) Be + $^{13}CH_4$, and (c) Be + CD_4.

methane (Matheson), $^{13}CH_4$ (MSD Isotopes, 99 atom %), CD_4 (MSD Isotopes, 99 atom %), or CH_2D_2 (Cambridge Isotope Laboratories, 99 atom %) diluted with argon (99.995%, Air Products) to give 2% mixtures. Target metals of beryllium (Johnson-Matthey), magnesium (^nMg rod, Fisher; ^{26}Mg, 96%, Oak Ridge National Laboratory), and calcium (Alfa Inorganics) were employed. A CsI window at 10 ± 1 K was the substrate for co-deposition of the gas mixture, at a rate of approximately 2 mmol/h, with the metal atoms ablated using a Nd: YAG laser (1064 nm) focused (10 cm focal length) onto the rotating metal target. Laser energies ranged from 20 to 50 mJ/pulse. Infrared spectra were recorded at 0.5 cm^{-1} resolution and with an accuracy of ±0.1 cm^{-1} using a Nicolet 750 FTIR equipped with a liquid N_2-cooled MCTB detector. Photolysis of the cold deposit was carried out using the output from a 1000 W mercury arc passed through a water filter to absorb infrared radiation.

Density functional theory (DFT) calculations were performed using the Gaussian 94 program package with the BP86 functional and the 6-311G* basis sets for each atom.[21-23] The pure DFT functional has been shown to work well for other simple beryllium species, particularly for predicting observed vibrational frequencies.[11]

Results

The infrared spectra obtained when beryllium, magnesium, or calcium atoms are co-condensed with methane will be reported in turn.

Beryllium. Figure 1 shows the infrared spectrum obtained when laser-ablated beryllium atoms were co-condensed with a 2% methane/argon mixture. The intensity and number of the features in the spectrum bear witness to the high reactivity of the metal atoms under the conditions of laser ablation and suggest that several products have been formed. The spectra also show the presence of trace quantities of H_2O, CO_2, and CO,[24-26] along with simple hydrocarbon products, C_2H_2, C_2H_4, and C_2H_6, all produced in low concentrations.[27-29] The broad band at 617.2 cm^{-1} observed in the experiment employing CH_4, which shifts to 612.6 ($^{13}CH_4$) and 454.0 cm^{-1} (CD_4), indicates the presence of the methyl radical.[30] Bands arising from BeH and BeH_2 may be assigned by comparison with the earlier matrix study.[7] BeH is identified by a single band at 1971.0 cm^{-1} in experiments using CH_4 or $^{13}CH_4$; the deuterated diatomic gives a very weak band at 1477.5 cm^{-1} when CD_4 is used as the reagent gas. The BeH_2 molecule was observed through absorptions at 2159.6 and 696.8 cm^{-1} in both the CH_4 and $^{13}CH_4$ experiments, while BeD_2 gave rise to bands at 1674.4 and 531.7 cm^{-1} in experiments involving CD_4. The frequencies associated with all of these hydride species are within ±0.5 cm^{-1} of the

(18) Burkholder, T. R.; Andrews, L. *J. Chem. Phys.* **1991**, *95*, 8697−8709.

(19) Andrews, L.; Burkholder, T. R. *J. Phys. Chem.* **1991**, *95*, 8554−8560.

(20) Hassanzadeh, P.; Andrews, L. *J. Phys. Chem.* **1992**, *96*, 9177−9182.

(21) Gaussian 94, Revision B.1; Frisch, M. J.; Trucks, G. W.; Schlegel, H. B.; Gill, P. M. W.; Johnson, B. G.; Robb, M. A.; Cheeseman, J. R.; Keith, T.; Petersson, G. A.; Montgomery, J. A.; Raghavachari, K.; Al-Laham, M. A.; Zakrzewski, V. G.; Ortiz, J. V.; Foresman, J. B.; Cioslowski, J.; Stefanov, B. B.; Nanayakkara, A.; Challacombe, M.; Peng, C. Y.; Ayala, P. Y.; Chen, W.; Wong, M. W.; Andres, J. L.; Replogle, E. S.; Gomperts, R.; Martin, R. L.; Fox, D. J.; Binkley, J. S.; Defrees, D. J.; Baker, J.; Stewart, J. P.; Head-Gordon, M.; Gonzalez, C.; Pople, J. A.; Gaussian, Inc.: Pittsburgh, PA, 1995.

(22) McLean, A. D.; Chandler, G. S. *J. Chem. Phys.* **1980**, *72*, 5639−5648. Krishnan, R.; Binkley, J. S.; Seeger, R.; Pople, J. A. *J. Chem. Phys.* **1980**, *72*, 650−654.

(23) Becke, A. D. *Phys. Rev. A* **1988**, *38*, 3098−3100. Perdew, J. P. *Phys. Rev. B* **1986**, *33*, 8822−8824.

(24) Redington, R. L.; Milligan, D. E. *J. Chem. Phys.* **1963**, *39*, 1276−1284.

(25) DiLella, D. P.; Tevault, D. E. *Chem. Phys. Lett.* **1986**, *126*, 38−42.

(26) Nelander, B. *J. Phys. Chem.* **1985**, *89*, 827−830.

(27) Andrews, L.; Johnson, G. L.; Kelsall, B. J. *J. Phys. Chem.* **1982**, *86*, 3374−3380.

(28) Andrews, L.; Johnson, G. L.; Kelsall, B. J. *J. Chem. Phys.* **1982**, *76*, 5767−5773.

(29) Davis, S. R.; Andrews, L. *J. Am. Chem. Soc.* **1987**, *109*, 4768−4775.

(30) Milligan, D. E.; Jacox, M. E. *J. Chem. Phys.* **1967**, *47*, 5146−5156.
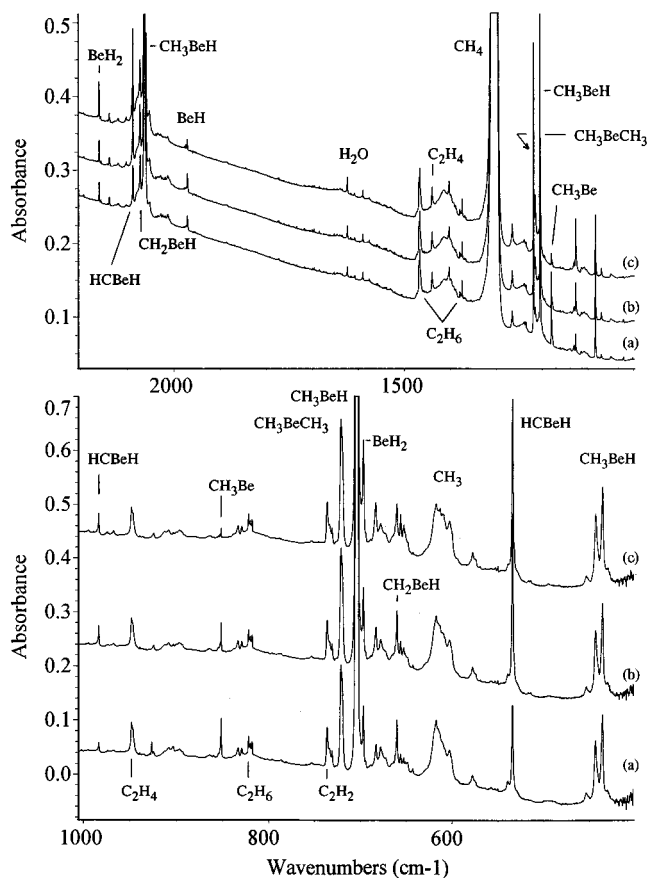
Figure 2. Infrared spectra of argon matrix following the co-deposition of laser-ablated Be atoms with 2% CH_4 in argon at 10 K: (a) sample deposited for 1 h at 10 K, (b) after 15 min photolysis with visible block filter, and (c) after final Pyrex filter and broad-band photolysis for 60 min each.

Table 1. Infrared Absorptions (cm^{-1}) Observed Following the Co-deposition of Laser-Ablated Beryllium Atoms with Methane/Argon Mixtures at 10 K

Be/$^{12}CH_4$/Ar	Be/$^{13}CH_4$/Ar	Be/CD_4/Ar	p/a[a]	assignment
2087.3	2086.4	1593.5	↑↑/↓	HCBeH
2071.9	2071.6	1578.2	↑/↓	CH_2BeH
2062.3	2062.1	1570.5	↑/↓	} CH_3BeH
2059.4	2058.9	1568.0		
1218.9	1206.3	b	↑/↓	CH_3BeCH_3
1205.4	1195.0	979.3	↑/↓	CH_3BeH
1180.6	1170.4	962.1	↓/↑	} CH_3Be
1178.9	1168.7			
1127.2	1123.6	1182.2	↑↑/↓	?
1084.1	1082.4	1154.4	↑/↓	} CH_3BeCH_3
1082.4	1080.6	1152.9		
983.7	970.7	935.2	↑↑/↓	HCBeH
924.6	914.7	837.1	↑/↓	CH_2BeH
851.7	843.8	765.6	↓/↑	CH_3Be
b	b	748.0	↑/↓	CH_3BeH
721.3	715.8	617.8	↑/↓	} CH_3BeH
720.1	714.4	615.8		
704.2	700.4	580.7	↑/↓	} CH_3BeH
		579.8		
682.8	678.6	555.9	↑/↓	?
660.0	654.2	541.8	↑/↓	CH_2BeH
534.2	533.0	430.2	↑↑/↓	} HCBeH
		427.8		
443.0	442.9	b	↑/↓	} CH_3BeH
435.4	435.3			

[a] Effects of photolysis (p)/annealing (a): large increase (↑↑), small increase (↑), or decrease (↓). [b] Corresponding bands were not observed.

values obtained for the molecules isolated in hydrogen-doped argon matrices.[7]

The remaining features may then be grouped together by their varying response to photolysis and annealing. The samples were irradiated initially using a visible block filter which removed light in the range of $400 < \lambda < 700$ nm, then a Pyrex filter (transmitting $\lambda > 290$ nm), and finally with broad-band light (220−1000 nm) from the full arc. Figure 2 contrasts the effect of visible blocked and subsequent broad-band photolysis. Thereafter, the deposit was subjected to a number of annealing cycles from base temperature to ca. 35 K.

For the experiments involving CH_4, a set of infrared features at 2062.3/2059.4, 1205.4, 704.2, and 443.0/435.4 cm^{-1} may at once be gathered together. All show a small increase in intensity of approximately 5% following an initial period of 15 min photolysis using the visible-block filter. Subsequent photolysis, as outlined above, continued this trend reaching a 10% growth as shown in Figure 2c after full-arc photolysis. Annealing the matrix caused these bands to decrease in intensity. The bands at 2062.3 and 704.2 cm^{-1} are the two most intense features in the spectrum after those attributable to CH_4, suggesting that they and the weaker features of the set are associated with the primary reaction product. Additional bands at 1218.9, 1084.1/1082.4, and 721.3/720.1 cm^{-1} displayed similar behavior but can be assigned to dimethylberyllium (vide infra).

Of the remaining infrared features, a set of bands at 2087.3, 983.7, and 534.2 cm^{-1} was characterized by an increase in intensity in the order of 50% following initial photolysis, while another set at 2071.9, 1388.5, and 660.0 cm^{-1} increased by

approximately 10%. Finally, bands at 1180.6/1178.9 and 851.7 cm^{-1} were made distinct by their reduction in intensity following photolysis and by being the only features in the spectrum to display growth following annealing of the matrix deposit.

The region of the spectrum 3100−2800 cm^{-1} associated with $\nu(C-H)$ revealed a number of features, including weak bands arising from C_2H_6. These features were also found, however, in experiments involving other metals[31] and so do not have their origin in a molecule containing beryllium. The absorptions observed at 1127.2 and 682.8 cm^{-1} remain unassigned.

The response of the infrared features described here to photolysis and annealing, along with the corresponding bands observed when $^{13}CH_4$ or CD_4 were used as the reagent gas, are listed in Table 1.

Magnesium. Experiments analogous to those previously described were performed using laser-ablated magnesium atoms. The resulting spectra are shown in Figure 3 for four isotopic samples. The reduced number and intensity of the new infrared features are indicative of the less reactive nature of the magnesium atom under the conditions of our experiments. Nevertheless, a set of absorptions was observed to increase in intensity following broad-band photolysis and to decrease when the matrix was subjected to annealing cycles up to 35 K; these occur at 1560.3/1552.2, 1127.7, and 547.9/545.4/542.8 cm^{-1}. Corresponding features were also observed in the experiments using $^{13}CH_4$ and CD_4 and when ^{26}Mg was employed as the target metal; these will be described in the Discussion. Observations in the higher frequency region, 3100−2800 cm^{-1}, paralleled those in experiments involving beryllium. The matrix was also found to contain the trace impurities and various hydrocarbon molecules observed in the beryllium experiments.

A band at 1421.7 cm^{-1} was observed in experiments using CH_4 or $^{13}CH_4$. This shifted to 1419.7 cm^{-1} when ^{26}Mg was the metal target and to 1037.4 cm^{-1} when CD_4 was the reagent gas. It indicates the presence of MgH identified in a previous

(31) Greene, T. M.; Andrews, L.; Downs, A. J. Unpublished results.
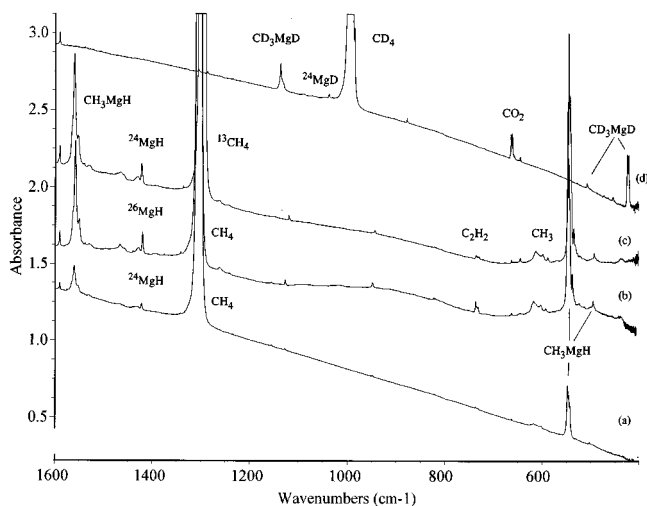
Figure 3. Infrared spectra of argon matrices following the co-deposition of laser-ablated Mg atoms with 2% methane/argon mixtures at 10 K: (a) Mg + CH_4, (b) ^{26}Mg + CH_4, (c) Mg + $^{13}CH_4$, and (d) Mg + CD_4.
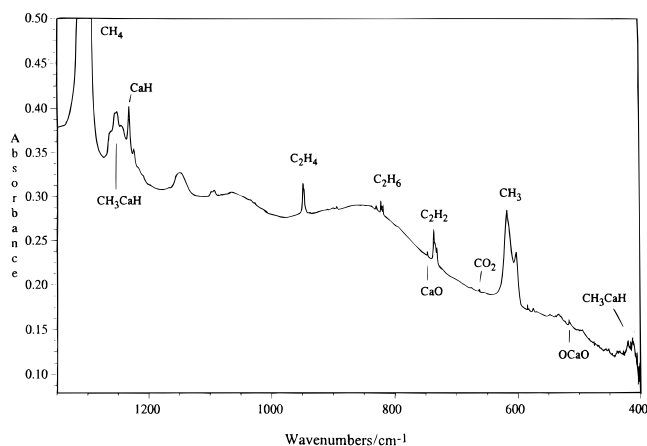
Figure 4. Infrared spectra of an argon matrix following the co-deposition of laser-ablated Ca atoms with 2% CH_4/argon mixture at 10 K.

matrix-isolation study of the reaction of laser-ablated magnesium atoms with dihydrogen.[14] The frequencies observed here are within ±0.4 cm^{-1} of those reported earlier. A very weak 1571.9 cm^{-1} band for the dihydride MgH_2 was detected. A number of other weak bands were observed to alter in intensity following photolysis. A sharp, weak band at 502.2 cm^{-1} exhibited isotopic counterparts but no associated bands could be located in these experiments. Such bands may well represent very small yields of molecules analogous to those found in the beryllium experiments (vide infra), but their reduced intensity prevents the identification of a sufficient number of absorptions to allow the carriers to be identified with confidence.

Calcium. The infrared spectrum of the matrix deposit following the co-condensation of laser-ablated calcium atoms with CH_4/Ar gas mixtures is shown in Figure 4. It is at once apparent that Ca atoms are much less reactive than Be or Mg atoms under similar conditions. In consequence, the spectrum displays few new features outside those signaling the presence of C_2H_2, C_2H_4, C_2H_6, and the CH_3 radical. Of these, a band at 1233 cm^{-1} may be assigned to the diatomic CaH, which has been observed in earlier studies examining the reaction of calcium atoms with dihydrogen in argon matrices and very weak sharp features at 747 and 516 cm^{-1} due to calcium oxides from target surface contaminants.[32] There then remains in the

spectrum broad features at 1263/1254/1245, 1151, 1098/1093, and 419/409 cm^{-1} which are unidentified. Broad-band photolysis did not bring about any changes in the infrared spectrum, while annealing altered only the relative intensities of features split by matrix-site effects. Experiments were also performed using neat methane in an attempt to increase the yield of any products formed. Although the spectra of these matrices did contain a number of new features, they were dominated by the presence of the hydrocarbons mentioned above, which result from the short-wavelength photolysis of the methane by the light emanating from the metal target.

Discussion

The infrared features observed in the experiments that have been described will be assigned to various organometallic products. A full justification of this assignment by way of a comparison with analogous species and with calculated vibrational properties will be presented. The mechanism leading to the formation of the observed products will then be discussed.

CH_3BeH. The group of frequencies associated with the primary reaction product are assigned to the monomethyl-beryllium hydride molecule, CH_3BeH. Calculations performed here and by others[33] suggest that such a molecule is linear at the metal and so possesses C_{3v} symmetry. For such a unit, eight infrared-active fundamentals are to be expected, four nondegenerate (a_1) and four doubly degenerate (e). Table 2 shows the excellent agreement between the frequencies observed for CH_3BeH and those forecast by DFT/BP86/6-311G* calculations. The occurrence of a pair of bands where only one fundamental is expected is the result of matrix splitting;[34] that it occurs for vibrations of both a_1 and e symmetry and is not consistent between the different isotopomers supports this argument, in preference to the possibility that a splitting of the degenerate e mode has been brought about by a bent geometry at the metal center. In addition to the frequencies given in Table 2, experiments involving CH_2D_2 led to the identification of features at 1567.1 (1582.0), 1120.3 (1144.5), and 597.2 (617.9) cm^{-1} associated with CH_2DBeD and at 2061.2 (2089.7), 1002.3 (1016.6), 660.1 (684.8), and 644.0 (667.6) cm^{-1} associated with CHD_2BeH (the calculated frequencies are given in parentheses). The descent in symmetry of these molecules from C_{3v} prevents their inclusion in Table 2.

As noted previously, we were unable to detect any $\nu(C-H)$ bands attributable to CH_3BeH either because of their inherently low intensity or, more probably, because of masking by the $\nu(C-H)$ bands of hydrocarbons present in the matrix deposit. Thus, the highest frequency that we can assign to CH_3BeH is 2062.3/2059.4 cm^{-1} which is clearly associated with $\nu(Be-H)$. This compares with values of 2119.4 and 2117.7 cm^{-1} for $\nu(Be-H)$ in HBeCCH[10] and HBeOH,[9] respectively. The frequency of the corresponding $\nu(Be-D)$ mode gives H/D ratios of 1.3131/1.3134, which is slightly lower than expected for a motion primarily involving the hydrogen atom (compare, for example, the case of CH_3MH (M = Zn, Cd, or Hg) where the ratio is ca. 1.39). The change reflects the participation of a much lighter metal atom. Of the fundamentals involving deformations of the CH_3 unit, only that arising from the symmetric deformation is observed, this being calculated to be

(32) Andrews, L.; Tague, T. J., Jr. Unpublished results. Andrews, L.; Yustein, J.; Thompson, C. A.; Hunt, R. D. *J. Phys. Chem.* **1994**, *98*, 6514–6512.

(33) Hashimoto, K.; Osamura, Y.; Iwata, S. *J. Mol. Struct. (THEOCHEM)* **1987**, *152*, 101–117.

(34) Barnes, A. J. In *Vibrational Spectroscopy of Trapped Species*; Hallam, H. E., Ed.; Wiley: London, 1973; Chapter 4.

Table 2. Observed and Calculated Frequencies (cm^{-1}) for CH_3BeH[a]

CH_3BeH		$^{13}CH_3BeH$		CD_3BeD		assignment	description of vibrational mode
obsd	calcd[a]	obsd	calcd[a]	obsd	calcd[a]		
b	2928.5 (2)[c]	b	2924.9 (2)	b	2107.2 (0.1)	$\nu_1 (a_1)$	ν_{sym}(C−H)
2062.3 / 2059.4	} 2090.9 (191)	2062.1 / 2058.9	} 2090.8 (190)	1570.5 / 1568.0	} 1581.5 (141)	$\nu_2 (a_1)$	ν(Be−H)
1205.4	1237.2 (151)	1195.0	1226.5 (48)	979.3	993.3 (42)	$\nu_3 (a_1)$	$\delta_{sym}(CH_3)$
b	854.0 (19)	b	845.1 (20)	748.0	745.3 (2)	$\nu_4 (a_1)$	ν(Be−C)
b	2991.0 (29)	b	2980.9 (31)	b	2207.7 (7)	$\nu_5 (e)$	ν_{asym}(C−H)
b	1422.7 (3)	b	1420.4 (3)	b	1026.9 (5)	$\nu_6 (e)$	$\delta_{asym}(CH_3)$
704.2	729.7 (376)	700.4	725.4 (374)	580.7 / 579.8	} 602.1 (257)	$\nu_7 (e)$	$\rho(CH_3)$
443.0 / 435.4	} 434.9 (65)	442.9 / 435.3	} 434.4 (64)	b	318.4 (31)	$\nu_8 (e)$	δ(C−M-H)

[a] Symmetry C_{3v}: C−H = 1.106 Å, C−Be = 1.679 Å, Be−H = 1.344 Å, ∠H−C−H = 112.6°. [b] Not observed. [c] Intensities (km mol^{-1}) are given in parentheses.

Table 3. Observed and Calculated Frequencies (cm^{-1}) for CH_3BeCH_3

CH_3BeCH_3			$^{13}CH_3Be^{13}CH_3$		CD_3BeCD_3			assignment	description of vibrational mode[d]
obsd[a]	obsd[b]	calcd[c]	obsd[a]	calcd[c]	obsd[a]	obsd[b]	calcd[c]		
1218.9	1222	1254.7 (167)	1206.3	1240.5 (154)	e	994	889.5 (2)	$\nu_6 (a_{2u})$	$\delta_{sym}(CH_3)$
1084.1 / 1082.4	} 1081	1095.4 (59)	1082.4 / 1080.6	} 1092.7 (65)	1154.4 / 1152.9	1150	} 1154.6 (204)	$\nu_7 (a_{2u})$	ν_{asym}(C−Be−C)
721.3 / 720.1	} 727	749.4 (251)	715.8 / 714.4	} 743.2 (246)	617.8 / 615.8	603	} 640.7 (206)	$\nu_{10} (e_u)$	$\rho(CH_3)$

[a] This work. [b] Values from gas phase, ref 36. [c] Intensities (km mol^{-1}) are given in parentheses; calculated bond lengths: C−H = 1.106 Å, C−Be = 1.685 Å. [d] There is an extensive interaction between ν_6 and ν_7 which is fully discussed in ref 40. [e] Band obscured by the ν_4 mode of CD_4.

the more intense. The position of $\delta_{sym}(CH_3)$ at 1205.4 cm^{-1} may be compared with a value of 1223 cm^{-1} obtained from the infrared spectrum of gaseous CH_3BeBH_4.[35] The next vibrational transition that the calculations suggest we should encounter approximating to ν(Be−C) is expected near 854 cm^{-1}. Although we do indeed see a band at 851.7 cm^{-1}, its behavior following photolysis and annealing of the deposit implies that it does not belong to the group of frequencies ascribed to CH_3-BeH. It seems most likely that this feature, which is assigned later, masks the ν(Be−C) band of CH_3BeH and so prevents its detection. Such a proposal is afforced by experiments involving CD_4 where we observe a band at 748.0 cm^{-1} attributable to the ν(Be−C) mode of CD_3BeD, along with another feature at 765.6 cm^{-1} which appears to be the counterpart of the band at 851.7 cm^{-1} observed in the CH_4 experiments. The final feature we may assign to the CH_3BeH molecule lies at 443.0/435.4 being associated with δ(C−Be−H). The corresponding band for the perdeuterated isotopomer is not observed; calculations suggest that it lies below 400 cm^{-1} and therefore beyond our range of detection.

CH_3BeCH_3. As stated earlier, bands at 1218.9, 1084.1/1082.4, and 721.3/720.1 cm^{-1} are assigned to dimethylberyllium, $(CH_3)_2Be$. This has been investigated in the gas phase,[36] with the conclusion that the unsaturated vapor contains only monomeric species. The infrared spectrum is reported to display strong features at 1222, 1081, and 727 cm^{-1} corresponding closely to the ones we observe for the matrix-isolated molecule. The assignments for the other isotopomers are made by reference to our DFT-calculated frequencies for $(^{13}CH_3)_2Be$ and to the gas-phase infrared spectrum of $(CD_3)_2Be$.[36] The bands we observe are compared with these other data in Table 3. The same features are also observed in experiments involving the co-deposition of ethane or CH_3Br with laser-ablated Be atoms.[37]

The formation of $(CH_3)_2Be$ by insertion of the metal atom into the C−C bond of ethane is noteworthy as neither copper[38] nor mercury[6] atoms have been observed to react in this way, both yielding C_2H_5MH (M = Cu or Hg). Studies of the reaction of metal atoms with ethane in the gas phase have led to the proposal that the stronger C−H bond is more susceptible to attack than is the weaker C−C bond because of the presence of a sufficient steric barrier opposing attack of the excited metal atom on the C−C bond.[15] It may well be that the much smaller Be atom can overcome such a barrier.

CH_3Be. A pair of infrared features is assigned in Table 1 to the radical CH_3Be. The DFT-calculated frequencies for this molecule are given in Table 4 and allow the assignment of the bands at 1180.6/1178.9 cm^{-1} to $\delta_{sym}(CH_3)$ and of the band at 851.7 cm^{-1} to ν(Be−C).

The species CH_3M (M = Li, Na, or K) have also been isolated in inert matrices.[39,40] The frequencies obtained for $\delta_{sym}(CH_3)$ are 1158, 1092, and 1053 cm^{-1}, a trend which has been interpreted, at least in part, in terms of an increasing charge separation between the metal and methyl group. The value we obtain at ca. 1178 cm^{-1} indicates a metal-to-carbon bond with significant covalent character. CH_3Be is presumably formed when the matrix is annealed by the reaction of Be atoms and CH_3 radicals as they diffuse together.

CH_2BeH. The set of bands at 2071.9, 1388.5, 660.0, and, possibly, 924.6 cm^{-1} increases by 10% following the first period of photolysis and decays by 20% over the rest of the photolysis sequence. This family is assigned on the basis of isotopic changes and DFT calculations to the radical CH_2BeH, as indicated in Table 5. The most intense band, at 660.0 cm^{-1}, is a CH_2 out-of-plane deformation mode as characterized by the observed 5.8 cm^{-1} [13]C and 118.2 cm^{-1} D shifts (to be compared

(35) Cook, T. H.; Morgan, G. L. *J. Am. Chem. Soc.* **1970**, *92*, 6487−6492.

(36) Kovar, R. A.; Morgan, G. L. *Inorg. Chem.* **1969**, *8*, 1099−1103.

(37) Lanzisera, D. V.; Andrews, L. Unpublished results.

(38) Ozin, G. A.; Mitchell, S. A.; García-Prieto, J. *Angew. Chem., Int. Ed. Engl.* **1982**, *21*, 211; *Angew. Chem. Suppl.* **1982**, 369−380.

(39) Andrews, L. *J. Chem. Phys.* **1967**, *47*, 4834−4842.

(40) Burczyk, K.; Downs, A. J. *J. Chem. Soc., Dalton Trans.* **1990**, 2351−2357.

Table 4. Observed and Calculated Frequencies (cm⁻¹) for CH₃Be

CH₃Be		¹³CH₃Be		CD₃Be		assignment	description of vibrational mode
obsd[a]	calcd[c]	obsd[a]	calcd[c]	obsd[a]	calcd[c]		
b	2922.4 (5)[c]	b	2919.0 (5)	b	2100.0 (1)	$\nu_1(a_1)$	$\nu_{sym}(\mathrm{C-H})$
1180.6 / 1178.9 }1205.7 (37)		1170.4 / 1168.7 }1195.4 (34)		962.1	985.1 (51)	$\nu_2(a_1)$	$\delta_{sym}(\mathrm{CH_3})$
851.7	855.7 (26)	843.8	847.2 (26)	765.6	773.8 (5)	$\nu_3(a_1)$	$\nu(\mathrm{Be-C})$
b	2992.8 (12)	b	2982.6 (16)	b	2210.1 (7)	$\nu_4(e)$	$\nu_{asym}(\mathrm{C-H})$
b	1412.9 (19)	b	1410.3 (18)	b	1021.2 (10)	$\nu_5(e)$	$\delta_{asym}(\mathrm{CH_3})$
b	558.8 (4)	b	555.3 (4)	b	433.4 (2)	$\nu_6(e)$	$\rho(\mathrm{CH_3})$

[a] Symmetry C_{3v}: C-H = 1.106 Å, C-Be = 1.688 Å, ∠H-C-Be = 112.0°. [b] Not observed. [c] Intensities (km mol⁻¹) are given in parentheses.

Table 5. Observed and Calculated Frequencies (cm⁻¹) for CH₂BeH

CH₂BeH		¹³CH₂BeH		CD₂BeD		assignment	description of vibrational mode
obsd	calcd[a]	obsd	calcd[a]	obsd	calcd[a]		
b	3005.4 (3)[c]	b	2999.4	b	2184.6	$\nu_1(a_1)$	$\nu(\mathrm{C-H})$
2071.9	2098.8 (178)	2071.6	2098.7	1578.2	1592.3	$\nu_2(a_1)$	$\nu(\mathrm{Be-H})$
1388.5	1375.3 (18)	1381.0	1369.0	b	1046.9	$\nu_3(a_1)$	$\delta(\mathrm{CH_2})$
b	924.8 (32)	b	912.7	b	827.3	$\nu_4(a_1)$	$\nu(\mathrm{Be-C})$
b	3070.6(10)	b	3059.2	b	2274.0	$\nu_5(b_1)$	$\nu(\mathrm{C-H})$
b	692.9 (183)	b	689.1	577.4	575.1	$\nu_6(b_1)$	$\delta(\mathrm{CH_2})$
(577.6)	508.4 (55)	(576.4)	508.3	b	385.4	$\nu_7(b_1)$	$\delta(\mathrm{C-M-H})$
660.0	658.5 (145)	654.2	652.3	541.8	542.7	$\nu_8(b_2)$	$\Delta(\mathrm{CH_2})$
b	419.1 (32)	b	418.6	b	305.8	$\nu_9(b_2)$	$\Delta(\mathrm{C-M-H})$

[a] Symmetry C_{2v}: C-H = 1.101 Å, C-Be = 1.656 Å, Be-H = 1.342 Å, ∠H-C-H = 125.0°. [b] Not observed. [c] Intensities (km mol⁻¹) are given in parentheses.

Table 6. Observed and Calculated Frequencies (cm⁻¹) for HCBeH[a]

HCBeH		H¹³CBeH		DCBeD		DCBeH		HCBeD		assignment	description of vibrational mode
obsd	calcd[a]	obsd	calcd[a]	obsd	calcd[a]	obsd	calcd[a]	obsd	calcd[a]		
b	3163.5 (0.3)	b	3153.0 (0.1)	b	2338.4 (4)	b	2339.6 (8)	b	3163.0 (0.2)	$\nu_1(\sigma^+)$	$\nu(\mathrm{C-H})$
2087.3	2113.8 (163)	2086.4	2113.7 (163)	1593.5	1608.0 (133)	2084.5	2111.8 (158)	1593.3	1610.8 (136)	$\nu_2(\sigma^+)$	$\nu(\mathrm{Be-H})$
983.7	998.3 (53)	970.7	983.1 (51)	935.2	926.5 (32)	961.7	976.5 (50)	947.1	946.7 (33)	$\nu_3(\sigma^+)$	$\nu(\mathrm{Be-C})$
534.2	526.4 (358)	533.0	525.1 (354)	430.2 / 427.8 }432.6 (228)		532.7	524.8 (169)	455.3	452.8 (116)	$\nu_4(\pi)$	$\delta(\mathrm{HCBeH})$
b	416.9 (12)	b	414.8 (14)	b	311.1 (1)	b	323.0 (5)	b	386.7 (9)	$\nu_5(\pi)$	$\delta(\mathrm{HCBeH})$

[a] Calculated for a linear geometry: H-C = 1.092 Å, C-Be = 1.621 Å, Be-H = 1.339 Å. [b] Not observed. [c] Intensities (km mol⁻¹) are given in parentheses.

with the calculated shifts of 6.2 and 115.8 cm⁻¹, respectively). The strong Be–H stretching mode shows a small ¹³C shift (0.3 cm⁻¹), even though the calculated shift is no more than 0.1 cm⁻¹. The CH₂ in-plane deformation mode is masked by the absorption of CH₃BeH, but the CD₂ counterpart is resolved at 577.4 cm⁻¹. Finally, a weak band at 577.6 cm⁻¹ occurs at a slightly higher than calculated frequency (508.4 cm⁻¹) but this mode is difficult to model; a tentative assignment is therefore appropriate.

HCBeH. Three absorptions with frequencies of 2087.3, 983.7, and 534.2 cm⁻¹ are grouped together by virtue of their marked growth following photolysis. The band at 2087.3 cm⁻¹ suggests the presence of a Be–H unit while that at 983.7 cm⁻¹ may be thought to arise from a $\nu(\mathrm{Be-C})$ mode. Calculations performed on HCBeH give infrared spectra in excellent agreement with the observed spectrum. The frequencies for HCBeH and its isotopomers are listed in Table 6. The molecule is calculated to be linear ($^3\Sigma^-$) in accord with a previous ab initio study where calculations were also reported for the ground state of the isomer H₂CBe.[41] The lowest energy structure ($^3B_1$) is reported to have C_{2v} symmetry. Although it is predicted that triplet H₂CBe lies some 12 kJ mol⁻¹ lower in energy than triplet HCBeH, a sufficient barrier (210 kJ mol⁻¹) is calculated to exist

(41) Luke, B. T.; Pople, J. A.; Schleyer, P. v. R. *Chem Phys. Lett.* **1983**, *97*, 265−269.

between the two molecules to suggest that both isomers are capable of existing independently. Our findings are at least in accord with this inasmuch as we have clearly identified the HCBeH molecule, but not, however, any features for the isomer H₂CBe.

CH₃MgH. The set of frequencies observed (Table 7) in experiments using laser-ablated magnesium atoms may readily be attributed to the insertion product CH₃MgH, by comparison both with the frequencies and intensity patterns generated by DFT calculations and with the infrared spectrum reported previously by McCaffrey et al.[13] for CH₃MgH isolated in solid methane. Again we were unsuccessful in assigning any frequencies to the $\nu(\mathrm{C-H})$ modes. As in the work with beryllium, the bands observed in this region were common to experiments employing a wide range of other metals, many of which do not yield monomethyl metal hydride species.[31] Our assigment of the bands at 1560.3/1552.2 cm⁻¹ to $\nu(\mathrm{Mg-H})$ and the perdeuterio shift to 1136.8 cm⁻¹ show excellent agreement with the calculated values. The discrepancies between the frequencies for CH₃MgH trapped in an argon and in a methane[13] matrix reflect the perturbing effects of the different matrix environments. The H/D ratio of 1.3725/1.3654 is considerably larger than that found for the same mode in CH₃BeH in keeping with the normal mode that involves principally motion of the hydrogen atom. Owing to the isolated $\nu(\mathrm{Mg-H})$ nature of this

Table 7. Observed and Calculated Frequencies (cm^{-1}) for CH$_3$MgH

	CH$_3$MgH			CH$_3$^{26}MgH		^{13}CH$_3$MgH			CD$_3$MgD			
	obsd[a]	obsd[b]	calcd[c]	obsd[a]	calcd[c]	obsd[a]	obsd[b]	calcd[c]	obsd[a]	obsd[b]	calcd[c]	assignment[d]
	e	2896	2928.3 (30)	e	2928.3 (30)	e	2896	2925.2 (30)	e	2036	2101.6 (12)	ν_1 (a_1)
	1560.3 1552.2	1524	1563.6 (273)	1558.3 1550.0	}1561.1 (271)	1560.4 1552.3	}1524	1563.6 (273)	1136.8	1115	1130.9 (156)	ν_2 (a_1)
	1127.7	1122	1159.4 (0.007)	1127.0	1159.4 (0.007)	1119.0	e	1151.8 (0.001)	877.1	872	892.2 (1)	ν_3 (a_1)
	e	539	526.2 (18)	537.8	518.9 (18)	534.5	528	515.7 (17)	506.9	424	489.2 (13)	ν_4 (a_1)
	e	2932	2998.6 (47)	e	2998.6 (47)	e	2924	2988.3 (48)	e	2190	2215.2 (12)	ν_5 (e)
	e	e	1435.2 (0.4)	e	1435.2 (0.4)	e	e	1432.4 (0.2)	e	e	1038.5 (3)	ν_6 (e)
	547.9 545.4 542.8	}550	581.5 (284)	547.2 544.8 543.0	}580.5 (280)	544.4 542.4 540.5	}546	577.8 (280)	423.8 422.9 421.1	}441	447.6 (195)	ν_7 (e)
	e	353 340	}298.5 (321)	e	297.6 (320)	e	350 340	}298.5 (322)	e	300 288	}219.2 (164)	ν_8 (e)

^{a} This work. ^{b} Data taken from ref 13. ^{c} Intensities (km mol^{-1}) are given in parentheses; symmetry C_{3v}: C–H = 1.105 Å, C–Mg = 2.106 Å, Mg–H = 1.725 Å, AH–C–H = 112.3°. ^{d} For the approximate description of the vibrational mode, see Table 2. ^{e} Not observed; see discussion.

mode, counterparts were slightly shifted (1560.1, 1138.4 cm^{-1}) in an experiment with CH$_2$D$_2$. In the same symmetry class, the symmetric methyl deformation was found at 1127.7 cm^{-1}.

Assignments of the fundamentals ρ(CH$_3$) and ν(Mg–C) will be taken together. Although the previous study of CH$_3$MgH[13] reported two features separated by 11 cm^{-1} which were identified with these modes, we were able to detect only a split band at 547.9/545.4/542.8 cm^{-1}. That this band obscures the presence of the ν(Mg–C) mode is made clear by isotopic substitution. Experiments involving either ^{26}Mg/CH$_4$ or Mg/^{13}CH$_4$ gave rise to a less intense band situated to low frequency of the main feature. This band shifts 3.3 cm^{-1} between CH$_3$^{26}MgH and ^{13}CH$_3$MgH in excellent agreement with the calculated shift for ν(Mg–C) of 3.2 cm^{-1}. That the separation of ρ(CH$_3$) and ν(Mg–C) is greater for ^{13}CH$_3$MgH than for CH$_3$-MgH is also supported by the experiments with methane matrices.[13] For the isotopomer CD$_3$MgD, we again observe a split band at 423.8/422.9/421.1 cm^{-1} arising from the ρ(CD$_3$) motion. In addition, a band at 506.9 cm^{-1} displays the appropriate behavior following photolysis and annealing for it to be assigned to CD$_3$MgD. The ratio of this frequency to that observed for ν(Mg–C) in CH$_3$^{26}MgH is 1.0610 in excellent agreement with the value of 1.0607 suggested by the calculations. As such, the band at 506.9 cm^{-1} is assigned to the ν(Mg–C) fundamental of CD$_3$MgD. In the previous study of CD$_3$MgD by McCaffrey et al.,[13] a band at 424 cm^{-1} was assigned to this mode, but incorrectly on the basis of the evidence of the present assignment. We note the importance of ^{26}Mg substitution for making the ν(Mg–C) vibrational assignment.

Additional experiments involving CH$_2$D$_2$ identified bands at 540.6 and 444.3 cm^{-1} to be associated with the molecule CH$_2$-DMgD, while a feature at 474.6 cm^{-1} is assigned to the isotopomer CHD$_2$MgH. These frequencies may be identified with fundamentals involving the methyl rocking mode.

CH$_3$CaH. Of the unidentified features in the Ca and CH$_4$ experiments the band at 1263/1254/1245 cm^{-1} may tentatively be assigned to the ν(Ca–H) mode and that at 419/409 cm^{-1} to the ρ(CH$_3$) mode of CH$_3$CaH. Comparison with the spectra of other CH$_3$MH species (M = Be or Mg) leads to the expectation that these two modes are the most intense in infrared absorption. Although it may be tempting to assign one of the remaining features at 1151 or 1098/1093 cm^{-1} to a ρ(CH$_3$) mode of CH$_3$-CaH, the relative intensities of these bands compared with that due to the ρ(CH$_3$) vibration warn against such an assignment. For CH$_3$MH (M = Zn,[6] Cd,[6] Hg,[6] Be, or Mg), these fundamentals are always much weaker in infrared absorption than is the methyl rocking mode. The absorptions at 1151 and 1098/1093 cm^{-1} must therefore remain unassigned.

Reaction Mechanisms. The signs are that CH$_3$BeH most likely results from the insertion of an energetically excited beryllium atom into a C–H bond of methane. The optical spectrum of Be atoms in a range of different matrices has been studied.[42] In argon the resonance transition $^1P_1 \leftarrow {}^1S_0$ appears at 236 nm while the spin-forbidden emission $^3P_1 \rightarrow {}^1S_0$ occurs at 465 nm. Laser ablation of the metal target populates both these states and imparts to the atoms sufficient kinetic energy to cause them to undergo insertion. Furthermore, the lifetime of the ^3P state is sufficient for a considerable population of the Be atoms to remain in this excited state and react in the condensing matrix.[43] The results of selective photolysis of the isolated reagents indicate that a Be atom excited to the $^1P_1$ state is capable of insertion, as is observed when the matrix is photolyzed using the visible block filter. However, additional growth of features attributable to CH$_3$BeH is also observed when photolysis with $\lambda > 290$ nm is employed. The absorption band $^1P_1 \leftarrow {}^1S_0$ for Be atoms is relatively sharp,[42] and so it seems most likely that the formation of CH$_3$BeH in the matrix can also be brought about by exciting Be atoms to their $^3P_1$ state. These findings are in accord with our mechanistic studies of the reaction of Zn, Cd, or Hg atoms with methane in argon matrices.[6]

In addition to CH$_3$BeH, we have identified a number of other products formed when Be atoms react with methane. Our knowledge of the behavior of these species in response to photolysis or to annealing allows us to suggest an overall reaction mechanism, Scheme 1. The first step of the reaction sequence involves the insertion of an excited Be atom into a C–H bond of methane, thereby generating CH$_3$BeH in an excited electronic state. This may in turn simply be quenched by interaction with the argon matrix to give CH$_3$BeH in its ground state or may decompose to yield the radicals BeH and CH$_3$. Furthermore, [CH$_3$BeH]* can decompose by H elimination to give the radical products CH$_3$Be and CH$_2$BeH or H$_2$ elimination to give HCBeH. The dramatic increase in the concentration of HCBeH following initial photolysis is the culmination of the photochemical reaction. The formation of CH$_3$BeCH$_3$ remains to be incorporated into this scheme; it is probably formed by the coming together of the radicals CH$_3$Be and CH$_3$. The CH$_3$ radical is present in the matrix either as a result of the decomposition of excited CH$_3$BeH or as a result of the high-energy photolysis of the methane molecule. The CH$_3$Be radical can also be formed on annealing from the union

(42) Brom, J. M., Jr.; Hewett, W. D., Jr.; Weltner, W., Jr. *J. Chem. Phys.* **1975**, *62*, 3122–3130.
(43) Andrews, L.; Chertihin, G. V.; Thompson, C. A.; Dillon, J.; Byrne, S.; Bauschlicher, C. W., Jr. *J. Phys. Chem.* **1996**, *100*, 10088–10099.

Scheme 1
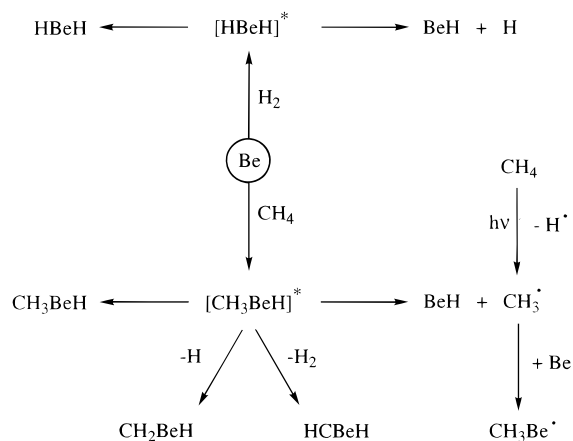
of a CH_3 radical and Be atom. Previous studies have shown that excited Be atoms react with dihydrogen to give BeH_2 and BeH,[8] molecules also present in these experiments.

The mechanism of the insertion process that yields CH_3MgH has been studied by McCaffrey et al. who have shown that photolysis at the $3p\ ^1P \leftarrow 3s\ ^1S$ Mg atom resonance absorption results in insertion of the metal into a C−H bond of methane.[43] Again the laser-ablation process produces an abundance of ^3P Mg atoms, which survive to react in the condensing matrix.[37]

It is noteworthy that the reduced tendency of the laser-ablated metals to form CH_3MH by insertion into a C−H bond of methane in the order Be > Mg > Ca correlates with the expected decrease in the metal−carbon bond strength. This also matches an increase in the relative yield of the decomposition

products MH (M = Be, Mg, or Ca) and CH_3. Any detailed understanding of the reasons for this reduction in reactivity is likely then to hinge on a full consideration of the energetics of the reaction, and the results of the present study invite a full computational analysis of the insertion process.

Conclusions

A matrix-isolation and density functional theoretical study of the reactions between laser-ablated beryllium, magnesium, or calcium atoms and methane has been performed. The insertion product CH_3MH (M = Be, Mg, or Ca) has been identified in each case by its infrared spectrum with the aid of isotopic substitution and also by comparison with the vibrational properties of other monomethyl metal hydrides. Selective photolysis studies have been employed in the case of beryllium to probe the mechanism of the reaction. This reaction yields, in addition to CH_3BeH, a range of other organoberyllium products, namely, $(CH_3)_2Be$, CH_3Be, CH_2BeH, and $HCBeH$, all of which were identified by the infrared spectra of their different isotopomers and density functional theory calculations of isotopic frequencies. The identities and structures of the species observed in our experiments were substantiated by the results of DFT/BP86 calculations.